JOURNAL OF GUIDANCE, CONTROL, AND DYNAMICS
Vol. 32, No. 3, May–June 2009

Semi-Analytical Solution for the Optimal Low-Thrust Deflection of Near-Earth Objects

Camilla Colombo,* Massimiliano Vasile,† and Gianmarco Radice‡
University of Glasgow, Glasgow, Scotland G12 8QQ, United Kingdom

DOI: 10.2514/1.40363

This paper presents a semi-analytical solution of the asteroid deviation problem when a low-thrust action, inversely proportional to the square of the distance from the sun, is applied to the asteroid. The displacement of the asteroid at the minimum orbit interception distance from the Earth's orbit is computed through proximal motion equations as a function of the variation of the orbital elements. A set of semi-analytical formulas is then derived to compute the variation of the elements: Gauss planetary equations are averaged over one orbital revolution to give the secular variation of the elements, and their periodic components are approximated through a trigonometric expansion. Two formulations of the semi-analytical formulas, latitude and time formulation, are presented along with their accuracy against a full numerical integration of Gauss equations. It is shown that the semi-analytical approach provides a significant savings in computational time while maintaining a good accuracy. Finally, some examples of deviation missions are presented as an application of the proposed semi-analytical theory. In particular, the semi-analytical formulas are used in conjunction with a multi-objective optimization algorithm to find the set of Pareto-optimal mission options that minimizes the asteroid warning time and the spacecraft mass while maximizing the orbital deviation.

Nomenclature

$\mathbf{A}_{\mathrm{MOID}}$	=	matrix form of proximal motion equations
$\mathbf{a}$	=	acceleration vector, km/s^2
a	=	semimajor axis, km
b	=	semiminor axis, km
d_m	=	diameter of the mirror, m
E	=	incomplete elliptic integral of the second kind
e	=	eccentricity
e_r	=	relative error
F	=	incomplete elliptic integral of the first kind
$\mathbf{G}_t$	=	matrix form of the Gauss equations
h	=	angular momentum, km^2/s
I_{sp}	=	specific impulse of the spacecraft engine, s
i	=	inclination, deg
j	=	integer number
k	=	proportionality constant of the acceleration, km^3/s^2
M	=	mean anomaly, deg
m_d	=	dry mass, kg
m_0	=	mass into space, kg
n	=	angular velocity, s^{-1}
p	=	semilatus rectum, km
r	=	orbital radius, km
$\mathbf{T}$	=	transition matrix
T_{NEO}	=	asteroid nominal orbital period, s or days
t	=	time, s
t_d	=	departure time from the Earth, s
t_e	=	time when the low-thrust arc ends, s
t_i	=	interception time, s
t_{MOID}	=	time at the minimum orbit interception distance point, s
t_w	=	warning time, s
$\mathbf{v}$	=	velocity vector, km/s
v	=	orbital velocity, km/s
$\boldsymbol{\alpha}$	=	vector of the orbital parameters
$\Delta\mathbf{r}$	=	vector distance of the asteroid from Earth at the minimum orbit interception distance, km
$\delta\mathbf{r}$	=	deviation vector in the Hill coordinate frame, km
δs	=	component of the deviation vector, km
$\delta\mathbf{v}$	=	impulsive maneuver vector, km/s
$\delta\boldsymbol{\alpha}$	=	orbital element difference between the perturbed and the nominal orbit
θ	=	true anomaly, deg
θ^*	=	argument of the latitude, deg
μ	=	sun gravitational constant, km^3/s^2
Ω	=	argument of the ascending node, deg
ω	=	argument of the perigee, deg

Subscripts

h	=	direction of the angular momentum
h	=	tangential direction in the orbital plane
n	=	normal direction in the orbital plane

I. Introduction

NEAR-EARTH-OBJECT (NEO) interception and hazard mitigation have been recognized as key issues for the safety of life on Earth. The threat posed by asteroid Apophis, with the uncertainties on its orbit after the close encounter with Earth in 2029, has highlighted the importance of space missions aiming at studying NEOs. In particular, tracking the position and velocity of the asteroid and characterizing its shape and composition have become of primary importance in view of any future deviation strategy. Furthermore, testing the technology required to deflect an asteroid is now the primary objective of missions such as Don Quijote [1].

The effect of a number of deviation strategies proposed in the past can be modeled as an impulsive variation of the velocity of the asteroid (e.g., kinetic impactor and nuclear explosion). Other strategies would instead result in a low thrust applied to the asteroid with a continuous momentum change (e.g., solar collector, pulsed

Received 11 August 2008; revision received 7 January 2009; accepted for publication 12 January 2009. Copyright © 2009 by Camilla Colombo, Massimiliano Vasile, and Gianmarco Radice. Published by the American Institute of Aeronautics and Astronautics, Inc., with permission. Copies of this paper may be made for personal or internal use, on condition that the copier pay the $10.00 per-copy fee to the Copyright Clearance Center, Inc., 222 Rosewood Drive, Danvers, MA 01923; include the code 0731-5090/09 $10.00 in correspondence with the CCC.

*Ph.D. Candidate, Department of Aerospace Engineering, James Watt (South Building); c.colombo@aero.gla.ac.uk. Student Member AIAA.

†Senior Lecturer, Department of Aerospace Engineering, James Watt (South Building); m.vasile@aero.gla.ac.uk. Member AIAA.

‡Senior Lecturer, Department of Aerospace Engineering, James Watt (South Building); g.radice@aero.gla.ac.uk. Member AIAA.

laser, mass driver, gravity tractor, and enhanced Yarkovsky effect) [2].

The consequent variation of the orbit of the asteroid can be computed through a numerical procedure, and the result has to be validated through orbit tracking and astronomical observations. Carusi et al. [3] studied the δv requirement for deflecting a hazardous near-Earth object at different epochs. The orbital course of the asteroid following a deflection impulse along its velocity is computed through the numerical propagation of the full n-body dynamics. They show that when an encounter occurs before the impact epoch, the required deflection maneuver is noticeably lower than after the encounter itself. Kahle et al. [4] extended this study by removing the assumption of a maneuver along-track; they showed that using a different direction for the deflection maneuver in the vicinity of a planetary encounter significantly increases the performance. The issue with numerical approaches is the computational time, which becomes a limit when the trajectory has to be integrated over a long period without losing accuracy. Of course, in the case of a real event, the CPU time would not be an issue; nonetheless, a number of authors have developed analytical formulations to make extensive investigations and gather useful lessons from the computation of a wide range of solutions. In this case, the simplification of the two-body problem is often adopted.

Ahrens and Harris [5] gave an estimation of the δv required for deflecting an asteroid from an Earth-crossing orbit, and Scheeres and Schweickart [6] derived an analytical expression of the shift in the position of the asteroid, under the assumption of a circular orbit and a constant acceleration aligned with the velocity of the NEO. This strategy, which yields a change in the mean motion of the asteroid, is proposed for when there is a long lead time until the impact. Subsequently, Izzo [7] proposed a similar solution, but extended to noncircular orbits. However, this formulation introduces an integral term that was solved analytically only in the case of an impulsive deflection maneuver. Furthermore, the effect of the deviation strategy is translated in a change of mean motion and hence in a phase shift; other changes in the orbital geometry are not included. A more general approach was used by Conway [8] to determine the near-optimal direction in which an impulsive maneuver should be given. The modified orbital course was propagated analytically forward in time by means of Lagrange coefficients expressed through universal formulas. An analysis on the minimum δv and the optimal impulse angle was performed by Park and Ross [9], who used Lagrange coefficients to propagate the deviated orbit of the asteroid rather than only its displacement with respect to the nominal course. They also included the effects of the Earth gravity [10,11]. Song et al. [12] investigated the deflection of asteroids and comets using a power-limited laser beam. They used the same technique proposed by Park and Ross [9] to solve the heliocentric two-body motion after the laser is shut off, whereas when the laser is on, the trajectory of the Earth-crossing object is numerically integrated. They found that the optimal operating angle between the asteroid velocity and the thrust acceleration vector remains in the range of 150–180 deg for warning times longer than one asteroid period, regardless of the orbital elements of the asteroid.

In this paper, the attention is focused on deviation techniques that make use of a continuous low-thrust action. In particular, we perform an extensive search for all mission opportunities over a wide range of launch dates that are Pareto-optimal with respect to three criteria: the achievable displacement of the asteroid at the point of minimum orbit interception distance (MOID), the time between the launch and the hypothetical impact, and the propellant mass for the transfer trajectory. Reconstructing the set of all Pareto-optimal solutions requires the evaluation of several tens of thousands of trajectories; thus, the numerical computation of the transfer trajectory of the spacecraft and of the deflected trajectory of the asteroid would be impractical.

Since 1950 [13–15], several authors have proposed analytical solutions to some particular cases of the low-thrust problem. Tsien [14] and Benney [15] developed a solution for escape trajectories, respectively, subject to radial and tangential continuous thrust acceleration. Following a similar formulation, Boltz [16,17] proposed a solution in case the ratio between the thrust and the gravity acceleration is kept constant. In both cases, the orbit is assumed to be circular or nearly circular.

Kechichian [18] used an averaging technique to compute analytical solutions for orbit-raising with constant tangential acceleration in the presence of Earth shadow. Kechichian's equations, which contain some terms expanded in power of the eccentricity, are accurate for small-to-moderate values of the eccentricity up to 0.2. The effects of the Earth oblateness are also considered. Gao and Kluever [19] adopted an averaging technique with respect to the eccentric anomaly for continuous-tangential-thrust trajectories, also accounting for the Earth oblateness and the Earth shadow. The value of the elliptic integrals in the solution of Gao and Kluever is approximated and the accuracy of the solution depends on the eccentricity.

Other analytical solutions for low-thrust trajectories were studied by Petropoulos [20], who presented a general overview of the approximated solutions derived so far. In his work, Petropoulos developed some analytical integrals to describe the secular evolution of the orbit of a spacecraft subject to different thrust control laws. The rate of change of the orbital energy and the eccentricity are time-averaged and reformulated, introducing some elliptic integrals, which are valid for all initial eccentricity from slightly above zero.

This paper proposes a semi-analytical approach to compute the displacement of the position of an asteroid at the MOID point after a low-thrust deviation maneuver and a shape-based approach for the transfer trajectory [21]. The miss distance achieved with a given deviation action is computed analytically by means of the proximal motion equations [22,23] expressed as a function of the orbital elements. The variation of the orbital parameters is then computed through Gauss planetary equations [24]. Note that the computation of the miss distance through proximal motion equations can be adopted for any deviation strategy and represents an extension and a generalization of the methodologies proposed in previous works [3,6,7] in which analytical formulas were derived to compute the deviation due to a variation in the orbital mean motion.

The assumption for the analytical developments in this paper is that the deflection strategy uses the sun as a power source, and therefore the thrust acceleration is inversely proportional to the square of the distance from the sun. Furthermore, we focus our attention on the case in which the thrust is aligned with the tangent to the osculating orbit of the asteroid.

To obtain an analytical solution for the variation of the orbital elements, Gauss equations are averaged over one orbital revolution. However, the required accuracy for the computation of the miss distance is higher than for the design of a generic low-thrust trajectory; hence, unlike other works [18–20], the periodic variation of the orbital elements is also taken into account. In addition, the analytic integrals are updated with a one-period step to further improve the accuracy. The general applicability of the proposed formulations and their accuracy is demonstrated through a number of test cases. Furthermore, some analyses are presented on the sensitivity of the deviation to the in-plane orbital elements of the nominal orbit of the asteroid. Finally, families of Pareto-optimal solutions for different asteroids will be presented.

II. Asteroid Deviation Problem

Given the time of interception t_i of a generic NEO, the objective is to maximize the minimum orbit interception distance from the Earth by applying a low-thrust deviation action, which consists of a continuous push on the asteroid's center of mass over a certain interval of time. In general, any deviation strategy generates a perturbation of the nominal orbit of the asteroid. The new orbit can be considered to be proximal to the unperturbed one (see Fig. 1).

If θ is the true anomaly of the NEO at the MOID along the unperturbed orbit and $\theta^* = \omega + \theta$ is the corresponding latitude, we can write the variation of the position of the NEO after deviation with

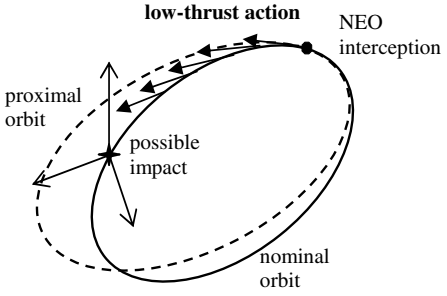

Fig. 1 Low-thrust deviation maneuver.

respect to its unperturbed position by using the proximal motion equations [22]:

$$\begin{aligned}
\delta s_r &\approx \frac{r}{a}\delta a + \frac{ae\sin\theta}{\eta}\delta M - a\cos\theta\delta e \\
\delta s_\theta &\approx \frac{r}{\eta^3}(1+e\cos\theta)^2\delta M + r\delta\omega \\
&\quad + \frac{r\sin\theta}{\eta^2}(2+e\cos\theta)\delta e + r\cos i\delta\Omega \\
\delta s_h &\approx r(\sin\theta^*\delta i - \cos\theta^*\sin i\delta\Omega)
\end{aligned} \tag{1}$$

where δs_r, δs_θ, and δs_h are the displacements in the directions that are, respectively, radial, transversal, and perpendicular to the orbit plane, so that the deviation is $\delta\mathbf{r} = [\,\delta s_r \quad \delta s_\theta \quad \delta s_h\,]^T$ and $\eta = \sqrt{1-e^2}$. In a matrix form,

$$\delta\mathbf{r}(t_{\mathrm{MOID}}) = \mathbf{A}_{\mathrm{MOID}}\delta\boldsymbol{\alpha} \tag{2}$$

where $\delta\boldsymbol{\alpha} = [\,\delta a \quad \delta e \quad \delta i \quad \delta\Omega \quad \delta\omega \quad \delta M\,]^T$ is the vector of the orbit element difference at the MOID between the perturbed and the nominal orbit, and M is the mean anomaly. When a low-thrust deviation action is applied over the interval $[\,t_i \quad t_e\,]$, where $t_e \leq t_{\mathrm{MOID}}$ is the time when the maneuver is ended, the total variation of the orbital parameters can be computed by integrating Gauss planetary equations [24]:

$$\begin{aligned}
\frac{\mathrm{d}a}{\mathrm{d}t} &= \frac{2a^2v}{\mu}a_t \\
\frac{\mathrm{d}e}{\mathrm{d}t} &= \frac{1}{v}\left[2(e+\cos\theta)a_t - \frac{r}{a}\sin\theta a_n\right] \\
\frac{\mathrm{d}i}{\mathrm{d}t} &= \frac{r\cos\theta^*}{h}a_h \\
\frac{\mathrm{d}\Omega}{\mathrm{d}t} &= \frac{r\sin\theta^*}{h\sin i}a_h \\
\frac{\mathrm{d}\omega}{\mathrm{d}t} &= \frac{1}{ev}\left[2\sin\theta a_t + \left(2e + \frac{r}{a}\cos\theta\right)a_n\right] - \frac{r\sin\theta^*\cos i}{h\sin i}a_h \\
\frac{\mathrm{d}M}{\mathrm{d}t} &= n - \frac{b}{eav}\left[2\left(1+\frac{e^2r}{p}\right)\sin\theta a_t + \frac{r}{a}\cos\theta a_n\right]
\end{aligned} \tag{3}$$

The low-thrust strategy provides an acceleration $\mathbf{a}(t) = [\,a_t \quad a_n \quad a_h\,]^T$, expressed here in a tangential-normal-binormal reference frame, such that a_t and a_n are the components of the acceleration in the plane of the osculation orbit, respectively, along the velocity vector and perpendicular to it, and a_h is the component perpendicular to the orbital plane. Note that the derivative of M in the sixth equation of system (3) takes into account the instantaneous change of the orbit geometry at each instant of time $t \in [\,t_i \quad t_e\,]$ and the variation of the mean motion due to the change in the semimajor axis along the thrust arc.

Letting $\boldsymbol{\alpha}(t) = [\,a \quad e \quad i \quad \Omega \quad \omega \quad M\,]^T$ be the vector of the orbital parameters, we define

$$\Delta\boldsymbol{\alpha} = \boldsymbol{\alpha}(t_e) - \boldsymbol{\alpha}(t_i) = [\,\Delta a \quad \Delta e \quad \Delta i \quad \Delta\Omega \quad \Delta\omega \quad \Delta M\,]^T$$

as the finite variation of the orbital elements with respect to the nominal orbit in the interval $[\,t_i \quad t_e\,]$, obtained from the numerical integration of Eqs. (3). It is important to point out that δM in Eqs. (1) must include the phase shift between the Earth and the asteroid. Therefore, because the mean anomalies at the MOID on the perturbed $\tilde{M}_{\mathrm{MOID}}$ and on the nominal orbits M_{MOID} are computed as

$$\begin{aligned}
\tilde{M}_{\mathrm{MOID}} &= M(t_e) + n_e(t_{\mathrm{MOID}} - t_e) = M(t_i) + \Delta M \\
&\quad + n_e(t_{\mathrm{MOID}} - t_e) = n_i(t_i - t_p) + \Delta M + n_e(t_{\mathrm{MOID}} - t_e) \\
M_{\mathrm{MOID}} &= n_i(t_{\mathrm{MOID}} - t_p)
\end{aligned}$$

where t_p is the passage at the pericenter, then the total variation in the mean anomaly between the proximal and the unperturbed orbit is

$$\delta M = \tilde{M}_{\mathrm{MOID}} - M_{\mathrm{MOID}} = (n_e - n_i)t_{\mathrm{MOID}} + n_i t_i - n_e t_e + \Delta M \tag{4}$$

where n_i is the nominal angular velocity and

$$n_e = \sqrt{\frac{\mu}{(a+\Delta a)^3}}$$

The variation of the other orbital parameters in Eqs. (1) is simply $\delta a = \Delta a$, $\delta e = \Delta e$, $\delta i = \Delta i$, $\delta\Omega = \Delta\Omega$, and $\delta\omega = \Delta\omega$.

If $\Delta\mathbf{r} = [\,\Delta s_r \quad \Delta s_\theta \quad \Delta s_h\,]^T$ is the vector distance of the asteroid from the Earth at the MOID and $\delta\mathbf{r} = [\,\delta s_r \quad \delta s_\theta \quad \delta s_h\,]^T$ is the variation given by Eqs. (1) at t_{MOID}, then the objective function for the maximum deviation problem is

$$\|\Delta\mathbf{r} + \delta\mathbf{r}\| = \sqrt{(\Delta s_r + \delta s_r)^2 + (\Delta s_\theta + \delta s_\theta)^2 + (\Delta s_h + \delta s_h)^2} \tag{5}$$

The proximal motion equations provide a very simple and general means to compute the variation of the MOID with good accuracy, without the need for further analytical developments. Compared with methods that analytically propagate the perturbed trajectory using Lagrange coefficients [9–12], the proposed approach does not require any solution of the time equation for every variation of the orbit of the asteroid and is therefore less computationally expensive. On the other hand, it is conceptually and computationally equivalent to those approaches [8] that analytically propagate only the variation of position and velocity of the asteroid by using the fundamental perturbation matrix [24]. Conversely, the benefit of using proximal motion equations expressed in orbital elements is the explicit relationship between the components of the perturbation action and the geometric characteristics of the orbit of the asteroid.

Gauss equations (3), together with Eq. (4), provide a way to compute the variation of the orbital elements between the nominal and the deviated orbits. The equations account for both the geometrical variation of the orbit and the secular change in the mean motion. To compute the effect of any low-thrust deflection strategy, Gauss equations would have to be numerically integrated. However, in Sec. III of this paper, we will restrict our attention to the case of a tangential push with the modulus inversely proportional to the square of the distance from the sun. Note that if we integrated only the first term of the last of Eqs. (3), neglecting the variations of e, i, ω, and Ω, and we inserted it into Eq. (4), we would get

$$\delta M = (n_e - n_i)t_{\mathrm{MOID}} + n_i t_i - n_e t_e + \int_{t_i}^{t_e} n\,\mathrm{d}t \tag{6}$$

which is the secular change in the mean motion, already considered by other authors [6,7]. The equivalence of Eq. (6) to what is already in the literature can be demonstrated as follows. Let us start by rewriting Eq. (6) as

$$\delta M = [n(t_{\mathrm{MOID}} - t)]_{t_i}^{t_e} + \int_{t_i}^{t_e} n\,\mathrm{d}t$$

and integrating by part

$$\delta M = \int_{t_i}^{t_e} (t_{\mathrm{MOID}} - t) \frac{\mathrm{d}n}{\mathrm{d}t}\, \mathrm{d}t \tag{7}$$

Now the differential $\mathrm{d}n$ can be written as a function of $\mathrm{d}a$, and through the first of Gauss equations (3) as a function of the time shift $\mathrm{d}t$:

$$\mathrm{d}\,n = \sqrt{\mu}\left(-\frac{3}{2}\right) a^{-5/2}\, \mathrm{d}a \qquad \mathrm{d}a = \frac{2a^2 v}{\mu} a_t\, \mathrm{d}t$$

Hence, Eq. (7) becomes

$$\delta M = -\frac{3}{\sqrt{\mu}} \int_{t_i}^{t_e} (t_{\mathrm{MOID}} - t) \frac{v}{\sqrt{a}} a_t\, \mathrm{d}t$$

If we now use the superscript $\wedge$ to denote the time coordinates measured from the interception time t_i and we take the mean value of the semimajor axis out of the integral, we get

$$\delta M = -\frac{3}{\sqrt{a\mu}} \int_0^{\hat{t}_e} (\hat{t}_{\mathrm{MOID}} - \hat{t}) < \mathbf{v}, \mathbf{a}(\hat{t}) > \mathrm{d}\hat{t}$$

which can then be translated from δM to the variation of the time to encounter, induced by the strategy deflection action $\mathbf{a}$, projected onto the velocity of the asteroid [7]:

$$\delta \tau = -\frac{3a}{\mu} \int_0^{\hat{t}_e} (\hat{t}_{\mathrm{MOID}} - \hat{t}) < \mathbf{v}, \mathbf{a}(\hat{t}) > \mathrm{d}\hat{t}$$

An estimation of the optimal direction [23] of the push can be obtained by maximizing the deviation $\|\delta \mathbf{r}\|$ at the MOID, given the time to impact $\Delta t = (t_{\mathrm{MOID}} - t_i)$. The deviation vector can be computed as

$$\delta \mathbf{r}(t_{\mathrm{MOID}}) = \mathbf{A}_{\mathrm{MOID}} \mathbf{G}_t \delta \mathbf{v}(t) = \mathbf{T} \delta \mathbf{v}(t)$$

where $\mathbf{T}$ is the transition matrix that links the impulsive $\delta \mathbf{v}$ at time t to the consequent deviation at t_{MOID}. $\mathbf{A}_{\mathrm{MOID}}$ is the matrix in Eq. (2) and $\mathbf{G}_t$ is the matrix associated with the Gauss equations written for finite differences; that is, the control acceleration is replaced by an instantaneous change in the asteroid velocity vector:

$$\delta \boldsymbol{\alpha} = \mathbf{G}_t \delta \mathbf{v}(t)$$

Following Conway's [8] approach, $\|\delta \mathbf{r}\|$ can be maximized by choosing an impulse vector $\delta \mathbf{v}_{\mathrm{opt}}$ parallel to the eigenvector of $\mathbf{T}$ conjugate to the maximum eigenvalue. As a result of this analysis, we can derive that for a Δt larger than a specific $\Delta t_{\mathrm{NEO}} < 1 T_{\mathrm{NEO}}$, the optimal impulse presents a dominant component along the tangent direction, and this one is associated with the shifting in time between the position of the asteroid and the Earth, rather than with a geometrical variation of the MOID. This conclusion is in agreement with the preliminary analysis on the $\delta \mathbf{v}$ direction performed by Ahrens and Harris [5], the numerical verification by Park and Ross [9], and the mathematical demonstration provided by Conway [8]. In the case of a low-thrust maneuver, as a first approximation, these results can be generalized by choosing the control vector at time t instantaneously tangent to the optimal impulsive $\delta \mathbf{v}(t)$. Hence, in this work, we focus on low-thrust acceleration in the tangent direction. This is a valid assumption when we consider hazardous cases with a warning time longer than approximately $0.75 T_{\mathrm{NEO}}$. For a better estimation of the optimal direction of thrust in the case of low-thrust propulsion, one can refer to the analysis by Song et al. [12].

Note that, in general, the direction that maximizes $\|\delta \mathbf{r}\|$ is not optimal for the maximization of $\|\Delta \mathbf{r} + \delta \mathbf{r}\|$ defined in Eq. (5). However, in this paper, we use the maximization of $\|\delta \mathbf{r}\|$ as an approximation to the general case, because it is valid for an actual impact (i.e., MOID equal to zero).

III. Semi-Analytical Formulas for Low-Thrust Deviation Actions

In this section, a set of semi-analytical formulas will be derived to calculate the total variation of the orbital parameters due to a low-thrust action. It is considered that a continuous acceleration a_t is applied along the orbit track, with the modulus given by

$$a_t = \frac{k}{r^2} \tag{8}$$

where r is the distance from the sun and k is a time-invariant proportionality constant that has to be fixed according to the specification of the power system. The selection of this acceleration law does not represent a severe restriction to the mission design; in fact, Eq. (8) describes any strategy that exploits the sun as a power source: for example, a solar electric propulsion spacecraft that rendezvouses with the NEO, anchors to its surfaces, and pushes or a solar mirror that collects the energy from the sun and focuses it onto the asteroid surface to ablate it. Moreover, if the formulas presented in the following are adopted to design a low-thrust trajectory, Eq. (8) represents the control acceleration due to a power-limited spacecraft.

Gauss equations are written as a function of the true latitude θ^*:

$$\frac{\mathrm{d}\boldsymbol{\alpha}}{\mathrm{d}\theta^*} = \frac{\mathrm{d}\boldsymbol{\alpha}}{\mathrm{d}t} \frac{\mathrm{d}t}{\mathrm{d}\theta^*}$$

where, in the case of zero-acceleration out-of-plane a_h,

$$\frac{\mathrm{d}\theta^*}{\mathrm{d}t} = \frac{h}{r^2} \tag{9}$$

where h is the orbital angular momentum. Under the hypothesis of planar tangential maneuver, Eqs. (3) become

$$\begin{aligned}
\frac{\mathrm{d}a}{\mathrm{d}\theta^*} &= \frac{2a^2 v}{\mu} \frac{r^2}{h} a_t \\
\frac{\mathrm{d}e}{\mathrm{d}\theta^*} &= \frac{1}{v} 2(e + \cos\theta) \frac{r^2}{h} a_t \\
\frac{\mathrm{d}i}{\mathrm{d}\theta^*} &= 0 \\
\frac{\mathrm{d}\Omega}{\mathrm{d}\theta^*} &= 0 \\
\frac{\mathrm{d}\omega}{\mathrm{d}\theta^*} &= \frac{1}{ev} 2 \sin\theta \frac{r^2}{h} a_t \\
\frac{\mathrm{d}M}{\mathrm{d}\theta^*} &= \left[n - \frac{b}{eav} 2 \left(1 + \frac{e^2 r}{p} \right) \sin\theta a_t \right] \frac{r^2}{h}
\end{aligned} \tag{10}$$

Equations (10) are averaged over one period of the true anomaly θ [24], yielding the average rate of change of the orbital parameters:

$$\left(\frac{\mathrm{d}\bar{\boldsymbol{\alpha}}}{\mathrm{d}\theta^*} \right)^{\theta, 2\pi} = \frac{1}{2\pi} \int_0^{2\pi} \frac{\mathrm{d}\boldsymbol{\alpha}}{\mathrm{d}\theta^*}\, \mathrm{d}\theta$$

The total variation $\Delta \bar{\boldsymbol{\alpha}}$ of the orbital elements over one orbital period of θ^* can be approximated as

$$\Delta \bar{\boldsymbol{\alpha}} \approx \int_0^{2\pi} \left(\frac{\mathrm{d}\bar{\boldsymbol{\alpha}}}{\mathrm{d}\theta^*} \right)^{\theta, 2\pi} \mathrm{d}\theta$$

if a zero variation in the anomaly of the pericenter is assumed (i.e., $\mathrm{d}\theta^* \approx \mathrm{d}\theta$). This assumption holds true when the deviation is calculated over one integer number of orbital revolutions, because the periodic variation of ω is zero and the secular one is of order 10^{-11} rad for the level of acceleration used in this paper. Thus, the variation of the orbital element over one revolution can be written as

$$\Delta\bar{e} = 2k\int_{\theta_0}^{\theta_0+2\pi}\frac{1}{h}\left((e+\cos\theta)\Big/\sqrt{\mu\left(\frac{1+e^2+2e\cos\theta}{a(1-e^2)}\right)}\right)\mathrm{d}\theta$$

$$\Delta\bar{a} = \frac{2k}{\mu}\int_{\theta_0}^{\theta_0+2\pi}\frac{a^2}{h}\sqrt{\mu\left(\frac{1+e^2+2e\cos\theta}{a(1-e^2)}\right)}\,\mathrm{d}\theta$$

$$\Delta\bar{i} = 0$$

$$\Delta\bar{\Omega} = 0$$

$$\Delta\bar{\omega} = 2k\int_{\theta_0}^{\theta_0+2\pi}\frac{\sin\theta}{eh}\sqrt{\frac{1}{\mu}\left(\frac{a(1-e^2)}{1+e^2+2e\cos\theta}\right)}\,\mathrm{d}\theta$$

$$\Delta\bar{M} = \int_{\theta_0}^{\theta_0+2\pi}\left(\frac{n}{h}\left(\frac{a(1-e^2)}{1+e\cos\theta}\right)^2 - \frac{2bk}{eah}\sin\theta\sqrt{\frac{1}{\mu}\left(\frac{a(1-e^2)}{1+e^2+2e\cos\theta}\right)} - \frac{2ebk}{ah}\frac{\sin\theta}{1+e\cos\theta}\sqrt{\frac{1}{\mu}\left(\frac{a(1-e^2)}{1+e^2+2e\cos\theta}\right)}\right)\mathrm{d}\theta$$

By considering a and e to be constant within one revolution, the following analytical formulas can be derived after some algebraic manipulations:

$$\Delta\bar{e} = \left[\frac{2k}{h}\frac{(1+e)\chi}{ev}\left((1+e)E\left[\frac{\theta}{2},\frac{4e}{(1+e)^2}\right] + (e-1)F\left[\frac{\theta}{2},\frac{4e}{(1+e)^2}\right]\right)\right]_{\theta_0}^{\theta_0+2\pi}$$

$$\Delta\bar{a} = \left[\frac{2a^2k}{\mu h}\left(2vE\left[\frac{\theta}{2},\frac{4e}{(1+e)^2}\right]\Big/\chi\right)\right]_{\theta_0,e_0}^{\theta_0+2\pi,e_0+\Delta\bar{e}}$$

$$\Delta\bar{i} = 0$$

$$\Delta\bar{\Omega} = 0$$

$$\Delta\bar{\omega} = \left[-\frac{2k}{eh}\frac{(1+e^2+2e\cos\theta)}{ev}\right]_{\theta_0,e_0}^{\theta_0+2\pi,e_0+\Delta\bar{e}}$$

$$\Delta\bar{M} = \left[2\arctan\left(\sqrt{\frac{1-e}{1+e}}\tan\left(\frac{\theta}{2}\right)\right) - \frac{e\sqrt{1-e^2}\sin\theta}{1+e\cos\theta} + \frac{2bk}{eah}\left(\frac{1+e^2+2e\cos\theta}{ve} + e\frac{2\arctan(v\sqrt{a}/\sqrt{\mu})\sqrt{1+e^2+2e\cos\theta}}{v\sqrt{1-e^2}}\right)\right]_{\theta_0,e_0}^{\theta_0+2\pi,e_0+\Delta\bar{e}} \tag{11}$$

where

$$v(\theta) = \sqrt{\mu\frac{1+e^2+2e\cos\theta}{a(1-e^2)}}$$

is the orbital velocity, and χ is defined as

$$\chi(\theta) = \sqrt{\frac{1+e^2+2e\cos\theta}{(1+e)^2}}$$

Equations (11) contain two elliptic integrals to be evaluated only once every orbital period:

$$F\left[\frac{\theta}{2},\frac{4e}{(1+e)^2}\right] \tag{12}$$

where

$$F[\phi,\lambda] = \int_0^{\phi}\frac{\mathrm{d}\varphi}{\sqrt{1-\lambda\sin^2\varphi}}$$

is the incomplete elliptic integral of the first kind and

$$E\left[\frac{\theta}{2},\frac{4e}{(1+e)^2}\right] \tag{13}$$

where

$$E[\phi,\lambda] = \int_0^{\phi}\sqrt{1-\lambda\sin^2\varphi}\,\mathrm{d}\varphi$$

is the incomplete elliptic integral of the second kind [24,25]. Note that the integral kernels (11) to be evaluated in $\theta_0+2\pi$ and θ_0 are only functions of the semimajor axis and the eccentricity.

The variation of the mean anomaly M strongly influences the consequent deviation, calculated through Eqs. (1). Hence, when the primitive function is evaluated in the upper limit $\theta_0+2\pi$, the value of the eccentricity is set equal to $e+\Delta\bar{e}$ to have a better approximation of $\Delta\bar{M}$ in Eqs. (11). This allows taking into account the secular variation $\Delta\bar{e}$ over one orbital revolution. Finally, the total variation of the orbital parameters over the thrust arc is determined by integrating Eqs. (11) with the Euler method with a step size of one orbital period.

The accuracy of Eqs. (11) is assessed by computing the relative error on the achieved deviation $\delta\mathbf{r}$ between the numerical propagation of Gauss equations and the analytical formulas:

$$e_r = \frac{\|\delta\mathbf{r}_{\text{propagated}} - \delta\mathbf{r}_{\text{analytical}}\|}{\|\delta\mathbf{r}_{\text{propagated}}\|}$$

The deviation $\delta\mathbf{r}$ is calculated considering a push of the asteroid over the angular interval $[\,\theta_0^* \quad \theta_0^*+j2\pi\,]$ with j an integer number and by calculating the resulting displacement right at the end of the thrust arc. The vector $\delta\mathbf{r}_{\text{analytical}}$ is the deviation obtained by means of the analytical formulas (11), and $\delta\mathbf{r}_{\text{propagated}}$ is computed through the numerical integration of Gauss's Eqs. (10):

$$\Delta\boldsymbol{\alpha} = \int_{\theta_0^*}^{\theta_0^*+j2\pi}\frac{\mathrm{d}\boldsymbol{\alpha}}{\mathrm{d}\theta^*}\,\mathrm{d}\theta^*$$

Figure 2a represents the relative error on the computation of the deviation of Apophis when pushing over an increasing number of orbital revolutions and starting the deviation maneuver at different angular positions. In fact, the variation of the orbital parameters over one orbital revolution depends on where the maneuver starts along the orbit. In the legend, t_p is the time at the pericenter, t_0 is the time when the deviation action commences, and T_{NEO} is the asteroid nominal orbital period. Figure 2b shows the relative error for an asteroid with higher eccentricity and inclination ($e=0.73$ and $i=25$ deg). An adaptive step-size Runge–Kutta Fehlberg integrator is used for the numerical integration, and the absolute and the relative tolerances are set to 1×10^{-16} and 2.3×10^{-14}, respectively, to obtain a relative error of the order of 10^{-5}. The value of k used for the following analyses is $k=2.2\times10^5$ km^3/s^2 for asteroid Apophis (Fig. 2a) and $k=2\times10^4$ km^3/s^2 for asteroid 1979XB (Fig. 2b). The reasons that led to these values will be explained in Sec. VI.

Other than the accuracy, an advantage of the analytical formulation is a significant reduction in the computational cost with respect to a numerical integration through a Runge–Kutta method. In fact, the CPU time[§] required for the numerical propagation of Gauss equations is 1 order of magnitude higher than that required for the computation of the analytical formulas, as reported in Table 1.

IV. Periodic Variation of the Orbital Parameters

The analytical formulation in Eqs. (11) describes the mean variation of the Keplerian elements; hence, it gives a sufficiently accurate estimate of their variation over one full revolution of the true

[§]Time calculated with a Pentium® 4 CPU at 3.00 GHz.

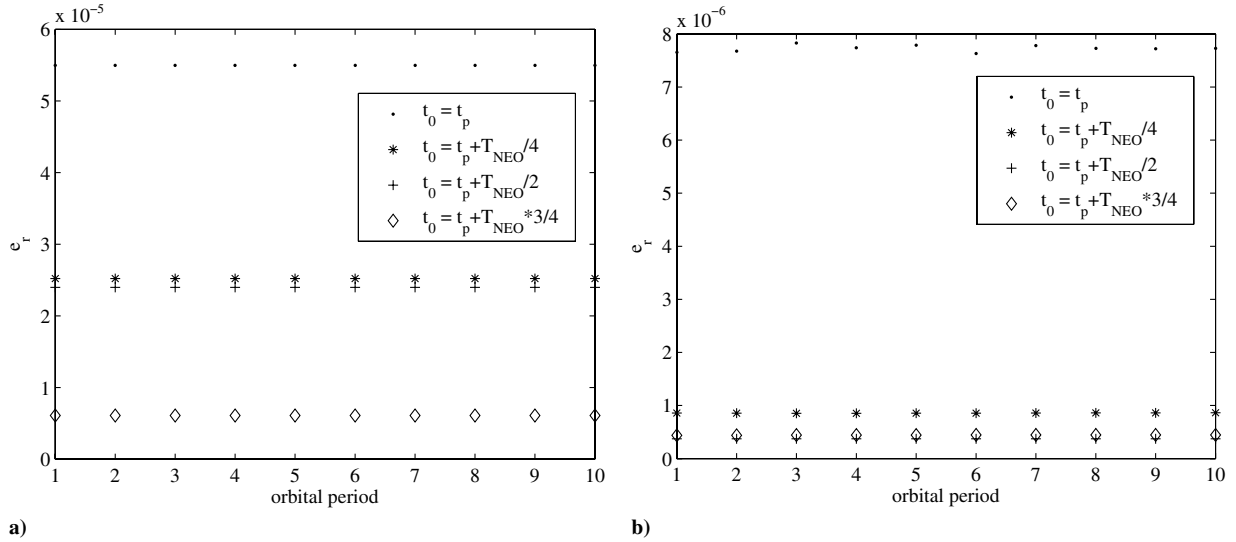

a) b)

Fig. 2 Relative error on the deviation: a) asteroid Apophis and b) asteroid 1979XB.

latitude. For smaller angular intervals, the periodic component of the perturbation must be included because its variation is not zero. To this aim, an expression is derived to estimate the periodic components of semimajor axis, eccentricity, and argument of the perigee. The trends of a, e, and ω functions of θ^* can be approximated by Eqs. (14):

$$
\begin{aligned}
a(\theta^*) &= a_0 - C_a \sin(\theta_0^* - \theta_p^*) + \frac{\Delta\bar{a}}{2\pi}(\theta^* - \theta_0^*) + C_a \sin(\theta^* - \theta_p^*) \\
e(\theta^*) &= e_0 - C_e \sin(\theta_0^* - \theta_p^*) + \frac{\Delta\bar{e}}{2\pi}(\theta^* - \theta_0^*) + C_e \sin(\theta^* - \theta_p^*) \\
\omega(\theta^*) &= \omega_0 + C_\omega \cos(\theta_0^* - \theta_p^*) + \frac{\Delta\bar{\omega}}{2\pi}(\theta^* - \theta_0^*) - C_\omega \cos(\theta^* - \theta_p^*)
\end{aligned}
\tag{14}
$$

where the first two terms are the initial condition for the secular evolution at point 0 (i.e., the point at which the deviation action commences), the third term indicates the secular variation obtained form Eqs. (11), and the fourth term is the periodic variation. The coefficients C_a, C_e, and C_ω are the amplitudes of the periodic variation. Their value is set through a calibration process: Gauss equations in Eqs. (10) are numerically integrated over one orbit of θ^*. With the vectors $\mathbf{a}_{\text{num},2\pi}$, $\mathbf{e}_{\text{num},2\pi}$, and $\boldsymbol{\omega}_{\text{num},2\pi}$ resulting from the numerical integration of Eqs. (10), we then have

Table 1 Computational time of the analytical and numerical approach

Orbital periods	Time analytical, s	Time numerical, s	Percentage of savings in computational time (analytical/numerical)
1	4.3e − 003	5.6e − 002	92.3
2	6.1e − 003	7.2e − 002	91.5
3	6.8e − 003	9.9e − 002	93.1
4	9.3e − 003	1.2e − 001	92.2
5	1.2e − 002	1.4e − 001	91.7
6	1.3e − 002	1.7e − 001	92.0
7	1.6e − 002	1.9e − 001	91.7
8	1.9e − 002	2.1e − 001	91.1
9	2.0e − 002	2.3e − 001	91.2
10	2.2e − 002	2.5e − 001	91.2

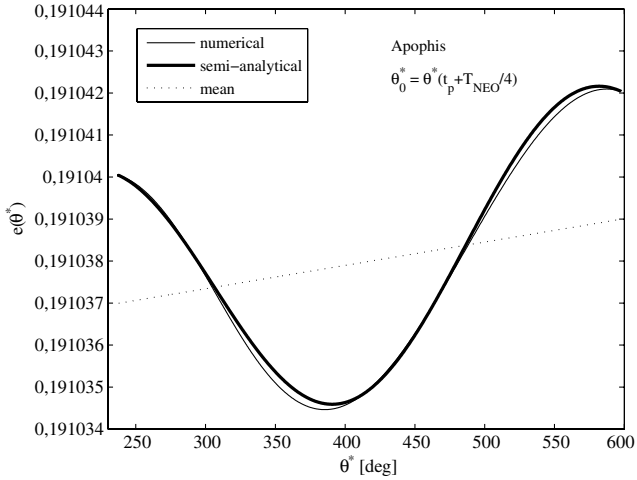

Fig. 3 Semi-analytical expression of the eccentricity for asteroid Apophis.

$$
\begin{aligned}
\underline{\mathbf{a}}_{2\pi} &= \mathbf{a}_{\text{num},2\pi} - \left(a_0 + \frac{\Delta\bar{a}}{2\pi}(\theta^* - \theta_0^*)\right) \\
\underline{\mathbf{e}}_{2\pi} &= \mathbf{e}_{\text{num},2\pi} - \left(e_0 + \frac{\Delta\bar{e}}{2\pi}(\theta^* - \theta_0^*)\right) \\
\underline{\boldsymbol{\omega}}_{2\pi} &= \boldsymbol{\omega}_{\text{num},2\pi} - \left(\omega_0 + \frac{\Delta\bar{\omega}}{2\pi}(\theta^* - \theta_0^*)\right)
\end{aligned}
\tag{15}
$$

from which the amplitudes of the periodic components can be computed as

$$
\begin{aligned}
C_a &= \frac{\max_{\theta^*}(\underline{\mathbf{a}}_{2\pi}) - \min_{\theta^*}(\underline{\mathbf{a}}_{2\pi})}{2} \\
C_e &= \frac{\max_{\theta^*}(\underline{\mathbf{e}}_{2\pi}) - \min_{\theta^*}(\underline{\mathbf{e}}_{2\pi})}{2} \\
C_\omega &= \frac{\max_{\theta^*}(\underline{\boldsymbol{\omega}}_{2\pi}) - \min_{\theta^*}(\underline{\boldsymbol{\omega}}_{2\pi})}{2}
\end{aligned}
\tag{16}
$$

where $\theta^* \in [\,\theta_0^* \quad \theta_0^* + 2\pi\,]$. Because Eqs. (15) come from a numerical integration, this calibration process is time-consuming. However, it needs to be performed once and for all, given the asteroid and the proportionality constant of the acceleration k. In fact, it is verified that for low-thrust action, the amplitude of the periodic

Table 2 Maximum relative error between the numerical and semi-analytical integration

	Asteroid Apophis	Asteroid 1979XB
Eccentricity	1.3e − 006	1.4e − 007
Semimajor axis	3.5e − 008	8.2e − 008
Anomaly of the pericenter	6.9e − 007	6.6e − 008

components of the perturbation is almost constant over a number of integration periods that are sufficient to deviate the asteroid by a considerable distance.

Through the calibration process, the second and fourth terms in Eq. (14) can be determined. The former term is required to find the initial condition for the secular variation of the orbital parameters. For example, Fig. 3 compares the semi-analytical expression of the eccentricity (bold solid line) with the numerical expression (solid line) for asteroid Apophis. The dashed line represents the mean variation. Table 2 summarizes the maximum of the relative error between the semi-analytical and the numerical integration of e, a, and ω, over 10 revolutions of θ^* for a low- (Apophis) and a high-elliptic asteroid (1979XB), respectively.

To properly take into account the periodic variation of the mean anomaly within an interval smaller than 1 revolution, the corresponding Gauss equation has to be integrated over θ^*:

$$\frac{\mathrm{d}M}{\mathrm{d}\theta^*} = \left[n - \frac{b}{eav} 2\left(1 + \frac{e^2 r}{p}\right) \sin\theta a_t \right] \frac{r^2}{h} \tag{17}$$

where $e(\theta^*)$, $a(\theta^*)$, and $\omega(\theta^*)$ are expressed through Eqs. (14). The relative error on M with respect to the full integration of Eqs. (10) is represented in Figs. 4a and 4b.

Note that introducing the periodic terms allows for the computation of the evolution of the orbital elements starting from any angular position along the orbit. In fact, if the point when the deviation action commences [i.e., point 0 in Eqs. (14)] is different from the pericenter, the initial mean parameters are different from the initial osculating elements. The periodic terms instead ensure the required accuracy for a deviation maneuver starting at any angular position. This would have not been achieved by using other formulations [18–20] that account only for the secular variations.

V. Time Formulation

In some applications, the semi-analytical formulas introduced in Secs. III and IV are enough to describe a low-thrust trajectory. The variation of the orbital parameters over an integer number of full revolutions of the angle θ^* can be calculated directly from Eqs. (11); for the last revolution, the periodic components are counted together with the secular variations through Eqs. (14). This approach, called *latitude formulation* in the following, does not use the time as an independent variable. It allows a considerable savings in computational time and, at the same time, it provides good accuracy, comparable with a numerical integration with low tolerance.

However, the time is required when dealing with the asteroid deviation problem, because the component of the deviation associated with the shift in time has to be taken into account. In fact, the latitude formulation accounts only for the shift in position of the

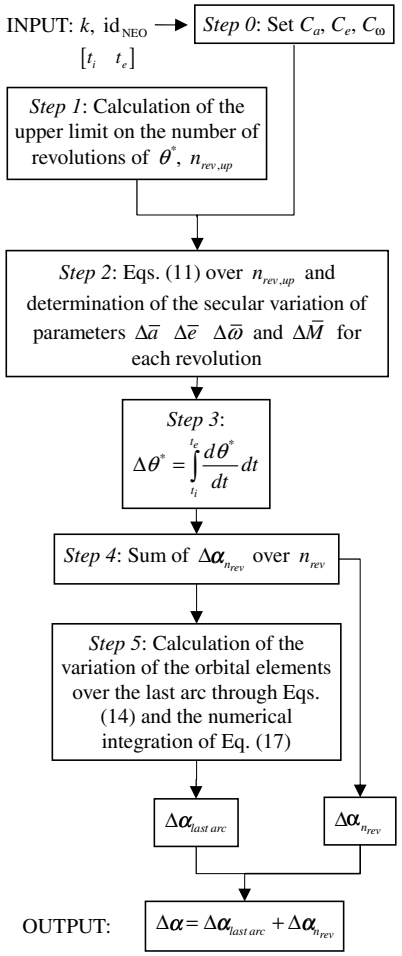

Fig. 5 Time-formulation algorithm.

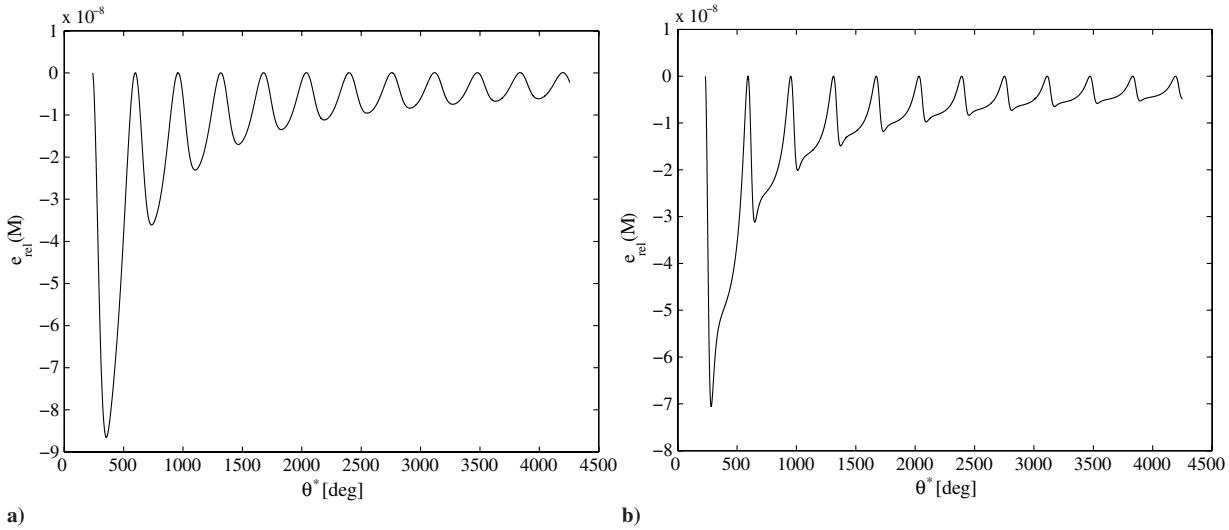

Fig. 4 Relative error between the numerical and semi-analytical integration of the mean anomaly: a) asteroid Apophis and b) asteroid 1979XB.

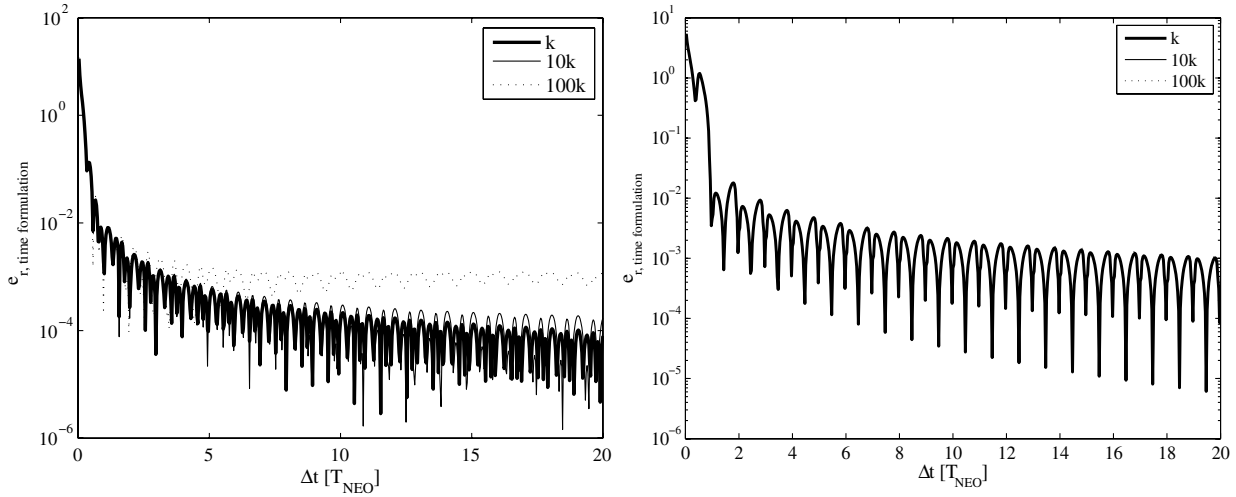

Fig. 6 Relative error of the time formulation: a) asteroid Apophis ($k = 2.2 \times 10^5\ \mathrm{km^3/s^2}$) and b) asteroid 1979XB ($k = 2 \times 10^4\ \mathrm{km^3/s^2}$).

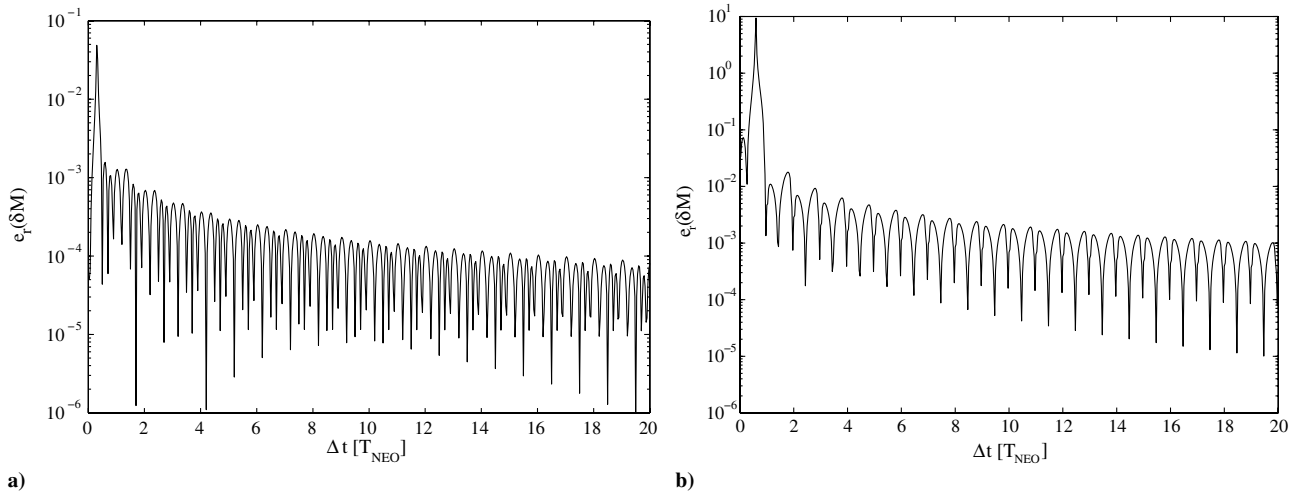

Fig. 7 Relative error on δM: a) asteroid Apophis and b) asteroid 1979XB.

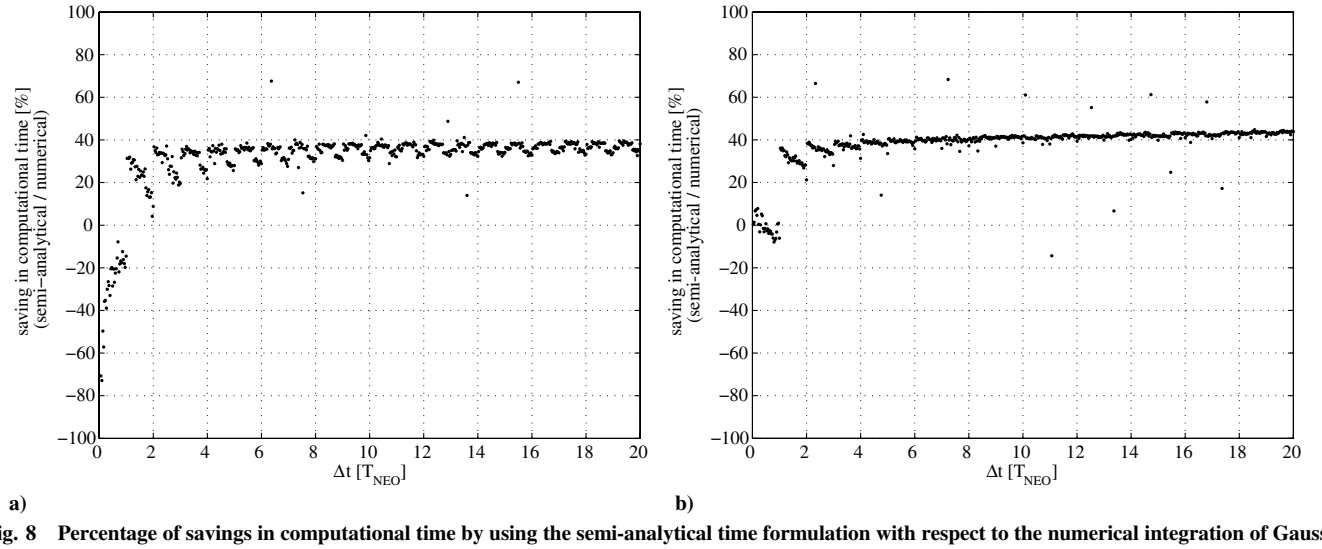

Fig. 8 Percentage of savings in computational time by using the semi-analytical time formulation with respect to the numerical integration of Gauss equations: a) asteroid Apophis and b) asteroid 1979XB.

Table 3 Asteroids orbital and physical parameters

Asteroid	Semimajor axis, AU	Eccentricity	Inclination, deg	MOID, km	Mass, kg
Apophis	0.922	0.191	3.331	30706	4.6×10^{10}
1979XB	2.350	0.726	25.143	3725733	4.4×10^{11}

Table 4 Mission characteristics

I_{sp}	3000 s
d_m	100 m
m_d	895 kg
Margin on m_0	25%
$v_{\infty,\max}$	3.5 km/s
$(t_{\text{MOID}} - t_d)_{\max}$	20 yr

asteroid. Given the thrust arc $[\,t_i \quad t_e\,]$, we want to apply the described semi-analytical formulation to find the displacement of the asteroid after a given time. Equations (11) are used to compute the variation of the orbital elements over the number of full revolutions contained in the time interval $[\,t_i \quad t_e\,]$. For the remainder of the thrusting arc, the element differences are calculated using Eqs. (14) and (17). The interval $\Delta\theta^*$ corresponding to the time interval $[\,t_i \quad t_e\,]$ is computed by numerically integrating Eq. (9). Note that the terms corresponding to the secular variation of the parameters in Eqs. (14) are calculated by updating $\Delta\bar{a}$, $\Delta\bar{e}$, and $\Delta\bar{\omega}$ at each orbital revolution.

Given the asteroid identification number id_{NEO} and the proportionality constant of the acceleration k, the calibration procedure gives the amplitude of the periodic components of a, e, and ω (step 0). Once computed, the values of C_a, C_e, and C_ω are kept constant for every $t \in [\,t_i \quad t_e\,]$ and for every interval $[\,t_i \quad t_e\,]$. The algorithm proceeds with the calculation of the upper limit on the number of revolutions contained in the interval $[\,t_i \quad t_e\,]$; the quotient of the division between $t_e - t_i$ and the nominal period of the asteroid is rounded to the nearest integer toward infinity (step 1). In fact, due to the perturbation introduced by the low-thrust action, the time to perform a full revolution of θ^* is different from that of the unperturbed orbit. For each revolution, the value of the secular variation of the orbital parameters is computed with Eqs. (11) (step 2), updating a and e at each integration step (which is one period long) and recalculating the elliptic integrals in Eqs. (12) and (13). Once the secular variations are available (step 3), the value of $\Delta\theta^*$ corresponding to the thrust arc and the exact number of revolutions are computed through Eq. (9), with the orbital parameters computed through Eqs. (14). The secular variations of the parameters calculated in step 2 are added up over the number of full revolutions (step 4), and the calculation of the variation of the orbital elements in the reminder of the thrust arc is performed through the evaluation of Eqs. (14) and the integration of Eq. (17) (step 5). Note that $a(\theta^*)$, $e(\theta^*)$, and $\omega(\theta^*)$, given by Eqs. (14), are calculated by updating the values of $\Delta\bar{a}$, $\Delta\bar{e}$, and $\Delta\bar{\omega}$ at each revolution. The output of the algorithm is the total variation of the orbital elements over the interval $[\,t_i \quad t_e\,]$. The overall process is sketched in Fig. 5.

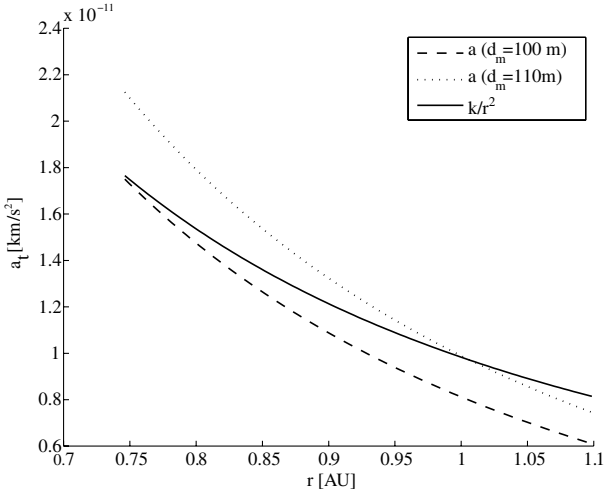

Fig. 9 Magnitude of the acceleration for Apophis.

The accuracy of the time formulation is verified by computing the relative error $e_{r,\text{time formulation}}$ between the deviation $\delta\mathbf{r}_{\text{analytical,tf}}$, calculated through the algorithm in Fig. 5, and the deviation $\delta\mathbf{r}_{\text{propagated,tf}}$, computed with the numerical integration of Eqs. (3):

$$e_{r,\text{time formulation}} = \frac{\|\delta\mathbf{r}_{\text{propagated,tf}} - \delta\mathbf{r}_{\text{analytical,tf}}\|}{\|\delta\mathbf{r}_{\text{propagated,tf}}\|}$$

The relative error is computed for increasing values of the proportionality constant k. Figures 6a and 6b report $e_{r,\text{time formulation}}$ calculated with the nominal value of k (set in Sec. VI), 10 and 100 k, respectively, for asteroids Apophis and 1979XB. The values of $e_{r,\text{time formulation}}$ are plotted against the push time $t_e - t_i$, which is set equal to the time to impact Δt (i.e., $t_e = t_{\text{MOID}}$).

The high value of the relative error when $\Delta t < 1T_{\text{NEO}}$ is due to the approximation introduced with the periodic components of the orbital elements in Eqs. (14). For $\Delta t < 1T_{\text{NEO}}$, the difference between orbital elements of the perturbed and the nominal orbit $\delta\boldsymbol{\alpha}$ is of the same order of magnitude of the approximation error of the periodic components. As a consequence, the relative error difference of the orbital elements

$$e_r(\delta\boldsymbol{\alpha}) = \frac{\delta\boldsymbol{\alpha}_{\text{propagated,tf}} - \delta\boldsymbol{\alpha}_{\text{analytical,tf}}}{\delta\boldsymbol{\alpha}_{\text{propagated,tf}}}$$

is high. In particular, the error on the assessment of the orbital parameters a, e, and ω affects the difference of mean anomaly, which significantly contributes to the terms in Eqs. (1). Figure 7 represents the relative error on δM for two asteroids.

Hence, the time formulation can be substituted to the numerical integration only for a thrust arc Δt longer than one orbital revolution. On the other hand, when low-thrust strategies are selected, the thrust arc is, in general, longer than 1 T_{NEO}. Figure 8 depicts the percentage of savings in computational time of the semi-analytical approach with time formulation, with respect to the numerical integration. When $\Delta t > 1T_{\text{NEO}}$, the gain is around 40%, and it increases with the length of the push arc.

VI. NEO Deviation Missions

In this section, the analysis of some NEO deviation missions is presented. Two asteroids are selected based on their orbital parameters: Apophis, with low eccentricity and inclination, and 1979XB, with high eccentricity and high inclination ($e = 0.7$ and $i = 25$ deg). The orbital elements that are most significant for the following analysis are reported in Table 3, together with the minimum orbit interception distance and the mass of the asteroid. The MOID Δr is calculated using the Earth's ephemerides on 27 January 2027 at 1200 hrs, taken from analytic ephemerides that approximate Jet Propulation Laboratory (JPL) ephemerides de405.¶ Note that the actual MOID varies with time [26], due to the actual orbit of both the Earth and the asteroid. On the other hand, the aim of this work is not to reproduce any specific and realistic impact scenario, but rather to assess the performance of a low-thrust deviation action over a wide range of mission opportunities. A more accurate calculation of the MOID would produce a more precise

¶Data available online at http://naif.jpl.nasa.gov/naif/pds.html [retrieved 28 January 2009].

Table 5 Acceleration constant and average of the accelerations acting on the asteroid

Asteroid	k, km^3/s^2	Average thrust acceleration, km/s^2	Average gravitational acceleration, km/s^2	Acceleration ratio
Apophis	2.2×10^5	1.2×10^{-11}	6.8×10^{-8}	1.7×10^{-4}
1979XB	2×10^4	3.5×10^{-13}	9.0×10^{-9}	3.9×10^{-5}

estimation of the actual achievable deviation, but would not invalidate the results in this paper.

As a reference case, we consider a spacecraft equipped with a solar mirror with a diameter of 100 m and a dry mass m_d [27] of 895 kg. The spacecraft is launched at a time t_d (selected in a range of 20 years before the possible collision, with maximum hyperbolic excess velocity of 3.5 km/s) and is equipped with an engine delivering an unlimited thrust with an $I_{sp} = 3000$ s. Once the spacecraft has intercepted the asteroid, the low-thrust deviation maneuver is performed from t_i up to the time at the MOID (i.e., $t_e = t_{\text{MOID}}$); no propellant is assumed to be consumed during the deviation phase, but a 25% margin on the total wet mass is considered, to account for stationkeeping and mirror deployment operations. Table 4 summarizes the key parameters of the mission.

The value of k is set according to the model of the solar collector developed in [28]. The value of k is chosen to obtain the same order of acceleration provided by a solar inflatable mirror, with a diameter d_m of between 100 and 110 m, along the range of distances from the sun covered by the asteroid during its motion. Figure 9 compares the acceleration computed through the full model described in [28] against Eq. (8) over a feasible range of distances for asteroid Apophis. Between the orbit apocenter and pericenter, Eq. (8) (solid line) gives an acceleration comparable with that calculated through the full solar collector model (dashed lines). Note that Eq. (8) does not take into account the decrease of the mass of the asteroid due to the ablation of the material.

Table 5 reports the values of the acceleration constant k for each asteroid, together with the average of the thrust acceleration on a nominal orbit of the asteroid, according to Eq. (8), the average of the sun gravitational acceleration and the ratio between the two accelerations.

A multi-objective optimization is performed to minimize the vector objective function:

$$\min([\, m_0 \quad t_w \quad -(\|\Delta\mathbf{r} + \delta\mathbf{r}\| - \|\Delta\mathbf{r}\|)\,]) \tag{18}$$

with respect to the launch date, the time of flight, and the hyperbolic excess velocity. In Eq. (18), m_0 is the wet mass at the Earth, defined as

$$m_0 = (m_d + m_p) \cdot 1.25$$

where m_p is the propellant mass for the transfer, $t_w = t_{\text{MOID}} - t_d$ is the warning time, and $\|\Delta\mathbf{r} + \delta\mathbf{r}\|$ is the total deviation to be maximized. The transfer trajectory is calculated through a shape-based method [21,29] and a hybrid optimization approach, blending a stochastic search with an automatic-solution space decomposition technique [30,31], is used for the solution of the problem in Eq. (18).

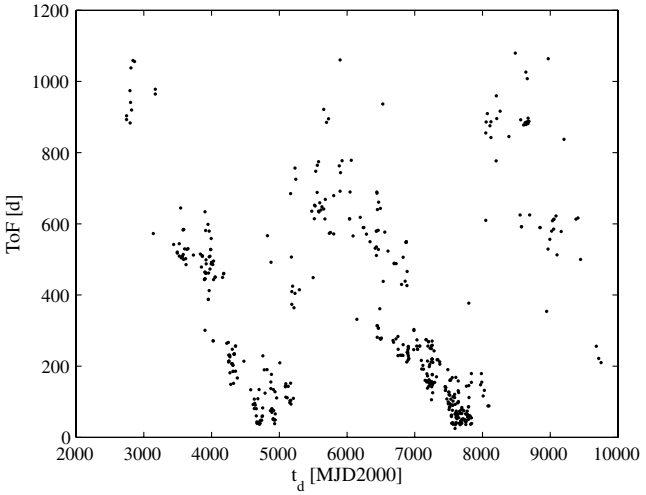

Fig. 10 Launch opportunities for a deviation mission to Apophis.

A. Apophis Deviation Mission

Figure 10 represents a set of launch opportunities for a deviation mission to Apophis, assuming that the asteroid is at the MOID on 7 July 2027 [10049 modified Julian date (MJD)2000]. Note that the Earth is not at the MOID on the same date, because the aim of these test cases is to measure the achieved deviation, not to reproduce a real impact scenario.

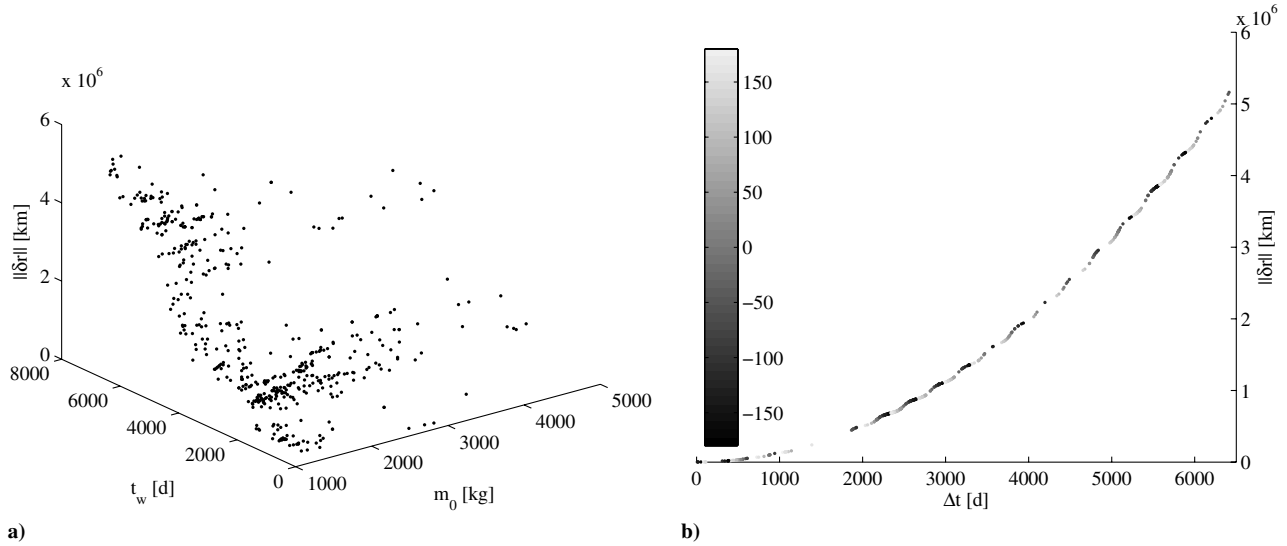

Fig. 11 Deviation mission to Apophis: a) Pareto-front, where launch mass, warning time, and magnitude of the deviation are represented on the three axes and b) achieved deviation as a function of the time length of the thrust arc.

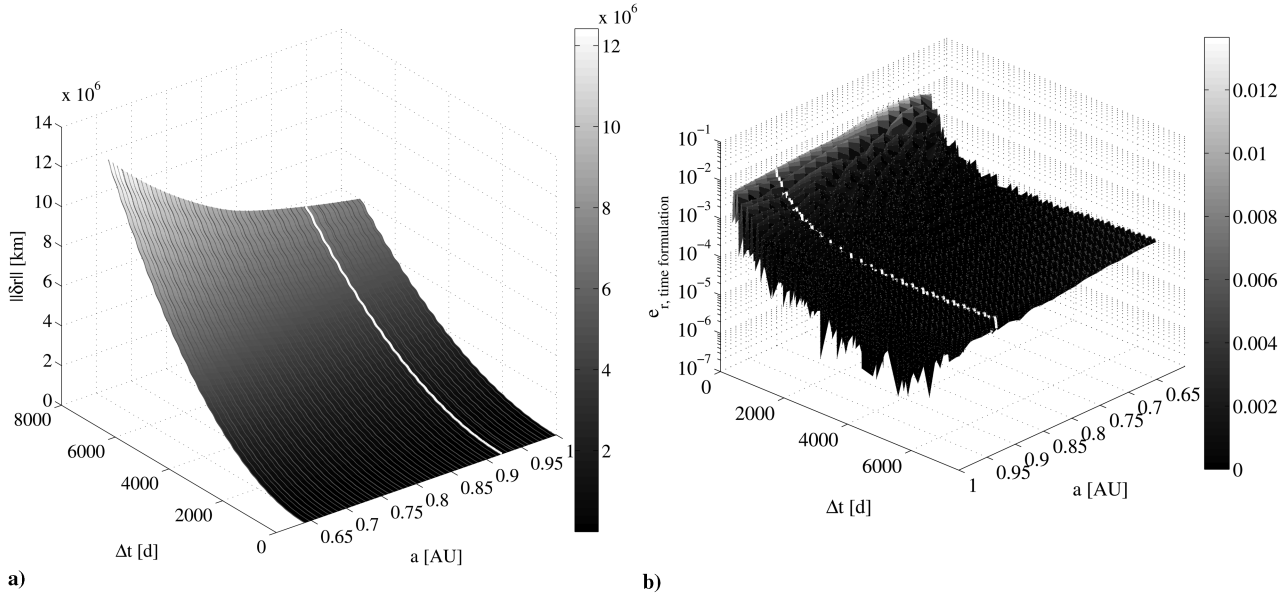

Fig. 12 Sensitivity of the deviation to the semimajor axis: a) deviation achieved for orbits with different values of semimajor axis and for increasing values of thrust interval and b) relative error for different values of semimajor axis. The white line represents the Apophis case ($a = 0.922$ AU).

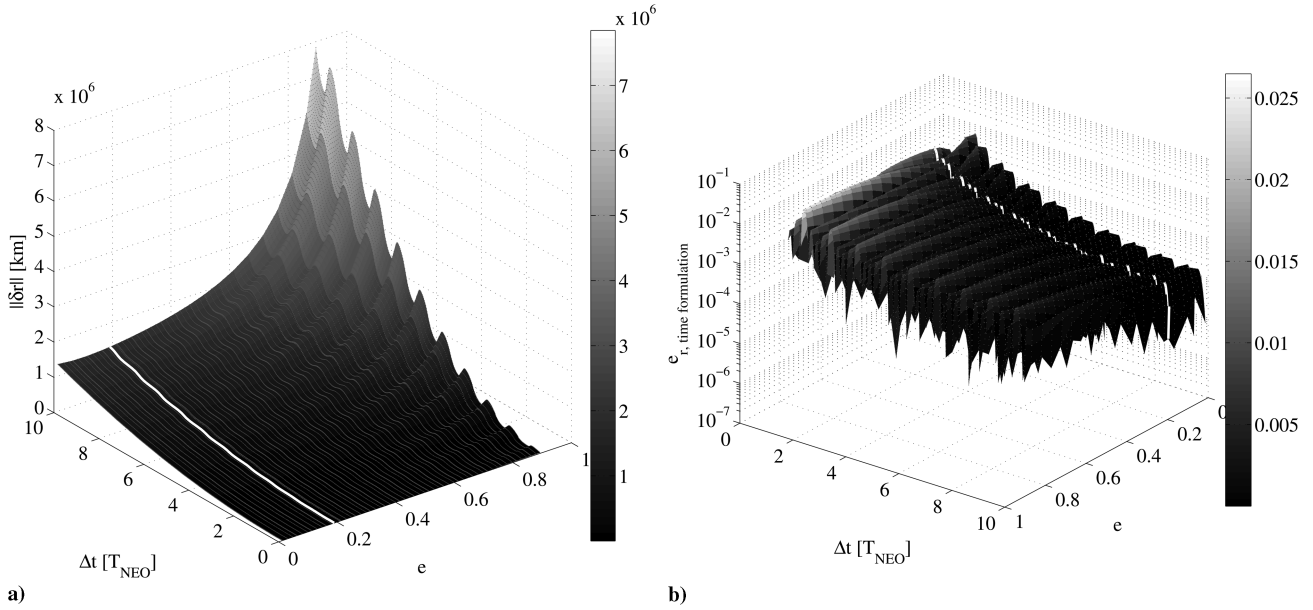

Fig. 13 Sensitivity of the deviation to the eccentricity: a) deviation achieved for orbits with different values of eccentricity and for increasing values of thrust interval and b) relative error for different values of eccentricities. The white line represents the Apophis case ($e = 0.191$).

The launch dates and transfer times in Fig. 10 correspond to the set of Pareto-optimal solutions in Fig. 11a. In Fig. 10, we can see that a wide range of launch opportunities are available every year between 2010 and 2030, though the required transfer time might change significantly. In particular, we can identify two groups of solutions around 5000 MJD2000 and 7500 MJD2000 with a short transfer time (i.e., short warning time), a scattered set of solutions with a transfer time between 500 and 600 days, and three groups of solutions with a long transfer time. Note that we used a nonexhaustive stochastic search process; therefore, more solutions can exist in the same range of launch dates. In Fig. 11a, the three axes represent the components of the objective function equation (18); the z axis contains the magnitude of the deviation $\|\delta\mathbf{r}\|$. The mass into space m_0, which is limited to 5000 kg in this analysis, is a function of the mass of propellant required to perform a transfer from the Earth to the asteroid. In the case of Apophis, a mission using a solar collector with a diameter of 100 m would achieve deviations of the order of 10^6 km, in a time range of 20 years of warning time, and solutions with 1000 days of warning time would have a deviation of about 20,000 km.

The modulus of the achieved deviation is proportional to the length of the thrust interval $\Delta t = t_{\text{MOID}} - t_i$ and it has a periodic trend with the angular position of the point of interception, as shown in Fig. 11b. The grayscale represents the value of the true anomaly (in degrees) at interception.

Neglecting the transfer phase and assuming the same value of the acceleration constant k, the sensitivity of the deviation to the in-plane orbital elements a and e of the nominal orbit of the asteroid can now be investigated. Several values of semimajor axis and eccentricity are considered, covering the range of in-plane elements for a group of 338 Aten asteroids from the JPL catalog.** The range for semimajor axis in astronomical units is $0.64 < a < 0.99$, and the range for eccentricity is $0.013 < e < 0.89$. For each value of eccentricity and

**Data available online at http://neo.jpl.nasa.gov/cgi-bin/neo_elem [retrieved 05 August 2008].

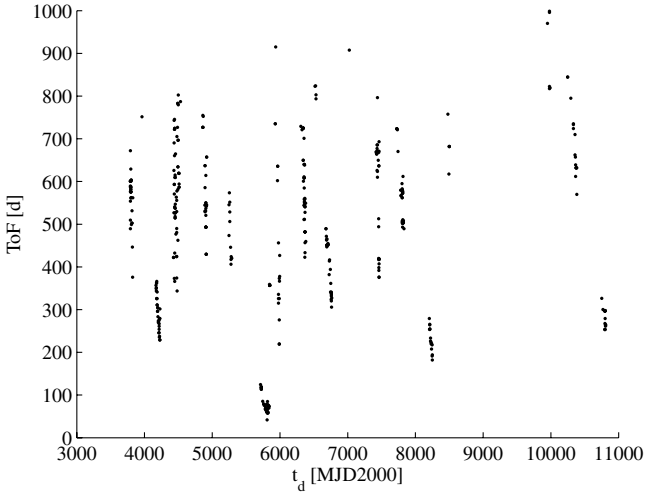

Fig. 14 Launch opportunities for a deviation mission to 1979XB.

semimajor axis, the corresponding orbit is computed by keeping the other orbital elements equal to the parameters of Apophis. The deviation is calculated for increasing values of the pushing time, from 1 day up to 20 years before the date at the corresponding MOID.

The modulus of the deviation of the asteroid at the MOID is displayed in Fig. 12a as a function of the pushing time. Note that as a consequence of the acceleration law, which goes with the inverse of the distance from the sun, the achievable deviation for a fixed warning time decreases with the increase of the nominal semimajor axis. This is clear if we analyze the first equation of Eqs. (3) and we substitute the value of the acceleration:

$$\frac{\mathrm{d}a}{\mathrm{d}t} = \frac{2a^2 v}{\mu}\frac{k}{r^2}$$

In fact, this term is proportional to $a^{-1/2}$ and is the term that most influences the value of the deviation, because it contributes to the shift in time.

As we can appreciate from Fig. 12b, the relative error with the precise numerical integration does not exceed 10^{-2}, which means

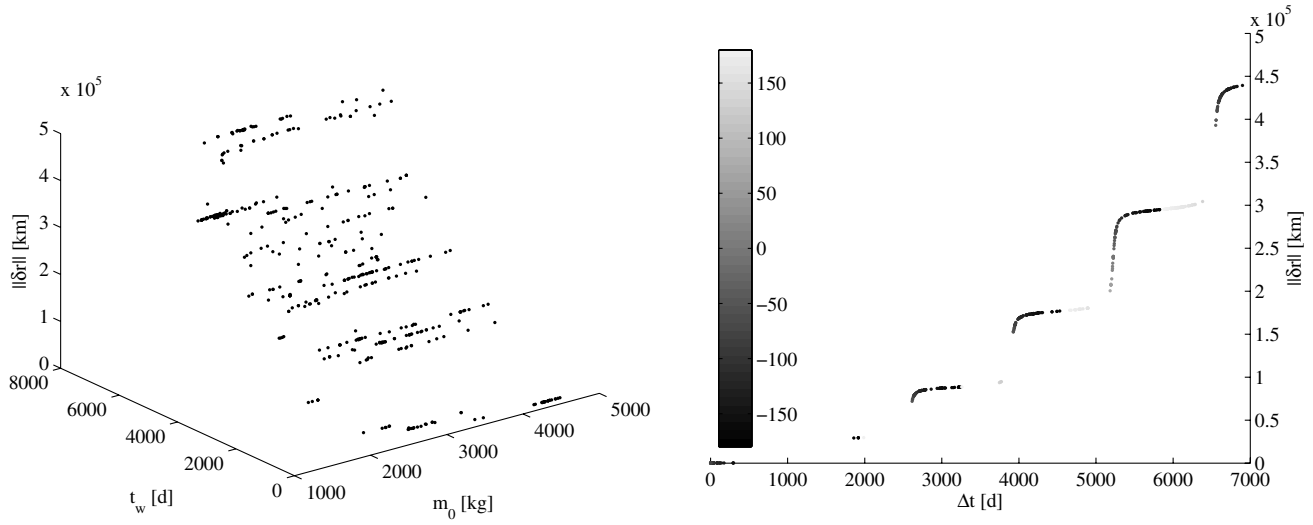

a) b)

Fig. 15 Deviation mission to 1979XB: a) Pareto front, where launch mass, warning time, and magnitude of the deviation are represented on the three axes and b) achieved deviation as a function of the time length of the thrust arc.

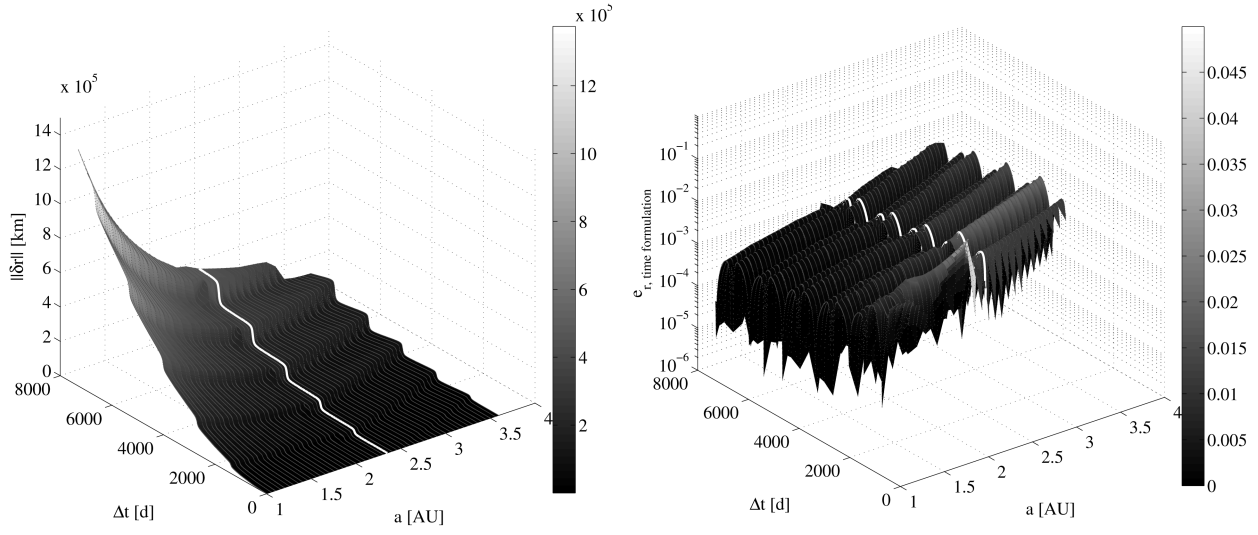

a) b)

Fig. 16 Sensitivity of the deviation to the semimajor axis: a) deviation achieved for orbits with different values of semimajor axis and for increasing values of thrust interval and b) relative error for different values of semimajor axis. The white line represents 1979XB case ($a = 2.350$ AU).

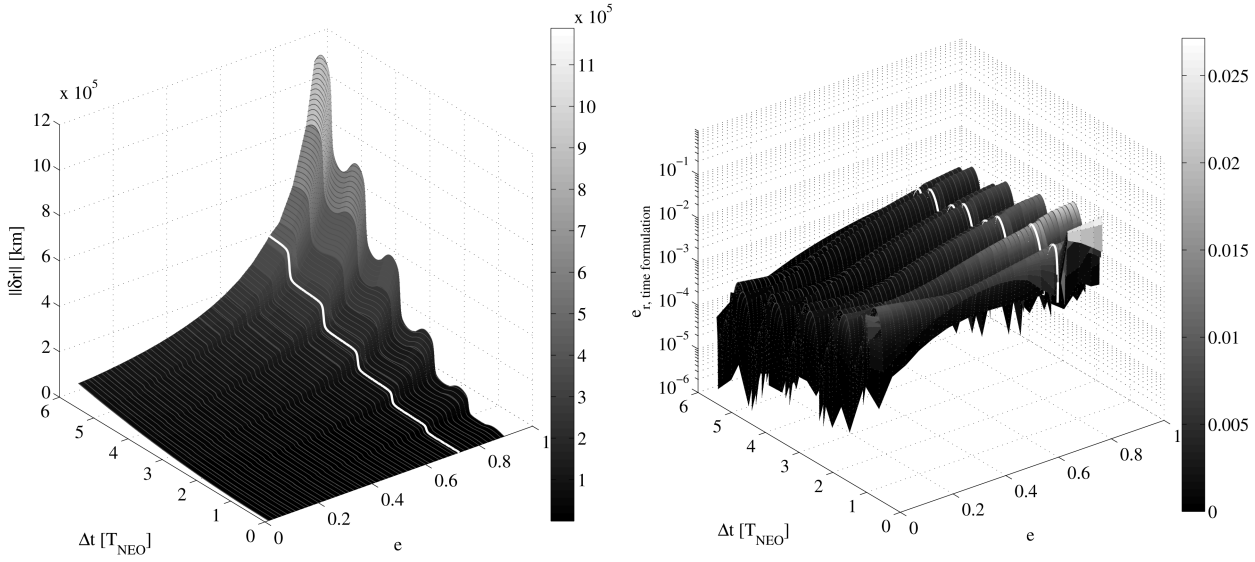

Fig. 17 Sensitivity of the deviation to the eccentricity: a) deviation achieved for orbits with different values of eccentricity and for increasing values of thrust interval and b) relative error for different values of eccentricity. The white line represents 1979XB case ($e = 0.726$).

that the accuracy of the analytical formulas is good in the selected range of values of the semimajor axis.

The sensitivity analysis to the eccentricity is shown in Fig. 13. In this case (see Fig. 13a), for the same pushing time, the magnitude of the deviation increases with the increase of the eccentricity. The fluctuations within the orbital period are also more visible. The local maxima correspond to an interception point before the pericenter.

Note that a good accuracy is also assured for different values of eccentricity within the range of $0.013 < e < 0.89$. Figure 13b shows the relative error of the time formulation. Note that the accuracy of the time formulation is, in general, lower than the accuracy of the latitude formulation. In fact, the former needs a further operation, which is the determination of the value of $\Delta\theta^*$ corresponding to the thrust arc and the exact number of revolutions (see step 3 in Fig. 5).

B. 1979XB Deviation Mission

The launch opportunities for a deviation mission to asteroid 1979XB are represented in Fig. 14. The test-case close approach occurs on 20 May 2030 (11097 MJD2000). In this case, the launch opportunities are grouped in single stripes, with an average transfer time ranging between around 200 and 800 days. The corresponding set of Pareto-optimal solutions is shown in Fig. 15a, which shows that the maximum achieved deviation is of the order of 10^5 km, because the mass of the asteroid is 4.4×10^{11} kg, significantly higher than the mass of Apophis.

The high eccentricity of the orbit of the asteroid 1979XB emphasizes the periodicity of the achievable deviation with Δt (see Fig. 15b, in which the grayscale indicates the angular position at interception). The considerable step in the value of the deviation is in correspondence of an interception before the pericenter. This effect is amplified for this asteroid, because its orbit is highly elliptical.

We performed the same analysis of sensitivity to the semimajor axis and the eccentricity by computing the deviation for a range of a and e and by keeping the other parameters equal to that of 1979XB, which belongs to the Apollo class. Although the range of the eccentricity is always $0.013 < e < 0.89$ for the semimajor axis, a range of $1.0006 < a < 3.595$ AU is considered as the range of semimajor axis of the Apollo class, taken from the JPL catalog (see footnote **).

Also in this case (see Fig. 16a), the value of the deviation for a fixed pushing time decreases with the increase of the semimajor axis (the 1979XB case is represented by a white line). The different shape with the orbital period with respect to Fig. 12a is due to the higher eccentricity ($e = 0.726$). Finally, the accuracy is represented in Fig. 16b. The relative error, despite being always under 3×10^{-2}, increases with the semimajor axis for fixed values of the pushing time.

The sensitivity to eccentricity is depicted in Fig. 17. As already observed in Fig. 13a, for the same pushing time, the magnitude of the deviation increases with the increase of the eccentricity (see Fig. 17a). Also in this case, a good accuracy is achieved for different values of eccentricity within the range of $0.013 < e < 0.89$. Figure 17b shows the relative error of the time formulation.

VII. Conclusions

In this paper, a solution to the asteroid deviation problem in the case of a low-thrust deviating action is proposed. Proximal motion equations are used to compute the achieved deviation at the minimum orbit interception distance, and semi-analytical formulas are derived to calculate the total variation of the orbital elements at the end of the thrust arc. The proposed semi-analytical formulation is proven to provide a significant savings in computational time with respect to the direct numerical integration of Gauss equations. In particular, for the anomaly formulation, the savings in computational time is up to 1 order of magnitude. The time formulation displays a lower savings, because the accuracy requirements are quite stringent for the specific application presented in this paper. Nonetheless, for very expensive calculations, such as the generation of the Pareto sets that require several hundreds of thousands of function evaluations, the semi-analytical formulas allow the generation of double the number of Pareto sets in the same computational time. Moreover, the gain in speed is not compensated by an equivalent loss in accuracy. The results in the paper show that the relative error on the variation of the orbital elements is small for a push interval longer than one orbital period and remains small for long spirals. On the other hand, for shorter periods, numerical integration has to be used because it is more accurate. Finally, the proposed semi-analytical formulas are accurate for a wide range of values for eccentricities, semimajor axis, and accelerations, suggesting their use for the fast generation of first-guess solutions for long escape or capture spirals.

The paper presents two applications of the semi-analytical formulation to the generation of sets of Pareto-optimal solutions for the design of mitigation missions to asteroids Apophis and 1979XB. For both asteroids, a wide range of launch opportunities are found between 2010 and 2030, with an achieved deviation that grows above the Earth–moon distance for warning times above 20 years. For shorter warning times, between 3 to 5 years, the achievable deviation is of the order of the radius of the geostationary orbit. The value of the achieved deviation presents a periodic trend with the true

anomaly of the interception point; in particular, when the eccentricity of the asteroid is high, an interception before the pericenter is significantly more effective than an interception after the pericenter.

References

[1] "A Reference Mission for Diminishing the Threat from Near-Earth Objects," ESA, TR CDF-39(A), Paris, Aug. 2005.

[2] "Near-Earth Object Survey and Deflection Analysis of Alternatives," NASA, Mar. 2007, http://neo.jpl.nasa.gov/neo/report2007.html [retrieved 27 January 2009].

[3] Carusi, A., Valsecchi, G. B., D'abramo, G., and Bottini, A., "Deflecting NEOs in Route of Collision with the Earth," *Icarus*, Vol. 159, No. 2, 2002, pp. 417–422. doi:10.1006/icar.2002.6906

[4] Kahle, R., Hahn, G., and Kührt, E., "Optimal Deflection of NEOs en Route of Collision with the Earth," *Icarus*, Vol. 182, No. 2, 2006, pp. 482–488. doi:10.1016/j.icarus.2006.01.005

[5] Ahrens, T. J., and Harris, A. W., "Deflection and Fragmentation of Near-Earth Asteroids," *Nature*, Vol. 360, No. 6403, Dec. 1992, pp. 429–433. doi:10.1038/360429a0

[6] Scheeres, D. J., and Schweickart, R. L., "The Mechanics of Moving Asteroids," 2004 Planetary Conference: Protecting Earth from Asteroids, Orange Country, CA, AIAA Paper 2004-1446, Feb. 2004.

[7] Izzo, D., "Optimization of Interplanetary Trajectories for Impulsive and Continuous Asteroid Deflection," *Journal of Guidance, Control, and Dynamics*, Vol. 30, No. 2, Mar.–Apr. 2007, pp. 401–408. doi:10.2514/1.21685

[8] Conway, B. A., "Near-Optimal Defection of Earth-Approaching Asteroids," *Journal of Guidance, Control, and Dynamics*, Vol. 24, No. 5, 2001, pp. 1035–1037. doi:10.2514/2.4814

[9] Park S.-Y., and Ross, I. M., "Two-Body Optimization for Deflecting Earth-Crossing Asteroids," *Journal of Guidance, Control, and Dynamics*, Vol. 22, No. 3, 1999, pp. 415–420. doi:10.2514/2.4413

[10] Ross, I. M., Park S.-Y., and Porter, S. D. V., "Gravitational Effects of Earth in Optimizing Δv for Deflecting Earth-Crossing Asteroids," *Journal of Spacecraft and Rockets*, Vol. 38, No. 5, Sept.–Oct. 2001, pp. 759–764. doi:10.2514/2.3743

[11] Park S.-Y., and Mazanek, D. D., "Mission Functionality for Deflecting Earth-Crossing Asteroids/Comets," *Journal of Guidance, Control, and Dynamics*, Vol. 26, No. 5, 2003, pp. 734–742. doi:10.2514/2.5128

[12] Song, Y.-J., Park, J.-Y., and Choi, K.-H., "Optimal Deflection of Earth-Crossing Object Using a Power Limited Spacecraft," 17th AAS/AIAA Space Flight Mechanics Meeting, Sedona, AZ, American Astronautical Society Paper 07-147, 2007.

[13] Lawden, D., "Rocket Trajectory Optimization: 1950–1963," *Journal of Guidance, Control, and Dynamics*, Vol. 14, No. 4, July–Aug. 1991, pp. 705–711. doi:10.2514/3.20703

[14] Tsien, H. S., "Take-Off from Satellite Orbit," *Journal of the American Rocket Society*, Vol. 23, No. 4, July–Aug. 1953, pp. 233–236.

[15] Benney, D. J., "Escape from a Circular Orbit Using Tangential Thrust," *Jet Propulsion*, Vol. 28, No. 3, Mar. 1958, pp. 167–169.

[16] Boltz, F., "Orbital Motion Under Continuous Radial Thrust," *Journal of Guidance, Control, and Dynamics*, Vol. 14, No. 3, May–June 1991, pp. 667–670. doi:10.2514/3.20690

[17] Boltz, F., "Orbital Motion Under Continuous Tangential Thrust," *Journal of Guidance, Control, and Dynamics*, Vol. 15, No. 6, 1992, pp. 1503–1507. doi:10.2514/3.56583

[18] Kechichian, J. A., "Orbit Raising with Low-Thrust Tangential Acceleration in Presence of Earth Shadow," *Journal of Spacecraft and Rockets*, Vol. 35, No. 4, July–Aug. 1998, pp. 516–525. doi:10.2514/2.3361

[19] Gao, Y., and Kluever, C. A., "Analytic Orbital Averaging Technique for Computing Tangential-Thrust Trajectories," *Journal of Guidance, Control, and Dynamics*, Vol. 28, No. 6, Nov.–Dec. 2005, pp. 1320–1323. doi:10.2514/1.14698

[20] Petropoulos, A. E., "Some Analytic Integrals of the Averaged Variational Equations for a Thrusting Spacecraft," *The Interplanetary Network Progress Report*, Jet Propulsion Lab., California Inst. of Technology, Rept. 42-150, Pasadena, CA, 2002, pp. 1–29.

[21] De Pascale, P., and Vasile, M., "Preliminary Design of Low-Thrust Multiple Gravity Assist Trajectories," *Journal of Spacecraft and Rockets*, Vol. 43, No. 5, Sept.–Oct. 2006, pp. 1065–1076. doi:10.2514/1.19646

[22] Schaub, H., and Junkins, J. L., *Analytical Mechanics of Space Systems*, AIAA Education Series, AIAA, Reston, VA, 2003, pp. 592–623.

[23] Vasile, M., and Colombo, C., "Optimal Impact Strategies for Asteroid Deflection," *Journal of Guidance, Control, and Dynamics*, Vol. 31, No. 4, July–Aug. 2008, pp. 858-872. doi:10.2514/1.33432

[24] Battin, R. H., *An Introduction to the Mathematics and Methods of Astrodynamics*, AIAA Education Series, AIAA, Reston, VA, 1999.

[25] Carlson, B. C., "Computing Elliptic Integrals by Duplication," *Numerische Mathematik*, Vol. 33, No. 1, 1979, pp. 1–16. doi:10.1007/BF01396491

[26] Valsecchi, G. B., Milani, A., Gronchi, G. F., and Chesley, S. R., "Resonant Returns to Close Approaches: Analytical Theory," *Astronomy and Astrophysics*, Vol. 408, No. 3, 2003, pp. 1179–1196. doi:10.1051/0004-6361:20031039

[27] Kahle, R., Kuhrt, E., Hahn, G., and Knollenberg, J., "Physical Limits of Solar Collectors in Deflecting Earth-Threatening Asteroids," *Aerospace Science and Technology*, Vol. 10, No. 3, 2006, pp. 256–263. doi:10.1016/j.ast.2005.12.004

[28] Sanchez, P., Colombo, C., Vasile, M., Radice, G., "Multi-Criteria Comparison Among Several Mitigation Strategies for Dangerous Near Earth Objects," *Journal of Guidance, Control, and Dynamics*, Vol. 32, No. 1, pp. 121–142, Jan.–Feb. 2009. doi:10.2514/1.36774

[29] Vasile, M., De Pascale, P., and Casotto, S., "On the Optimality of a Shape-Based Approach on Pseudo-Equinoctial Elements," *Acta Astronautica*, Vol. 61, 2007, pp. 286–297.

[30] Vasile, M., "Robust Mission Design Through Evidence Theory and Multiagent Collaborative Search," *Annals of the New York Academy of Sciences*, Vol. 1065, No. 1, Dec. 2005, pp. 152–173. doi:10.1196/annals.1370.024

[31] Vasile, M., "A Behavioral-Based Meta-Heuristic for Robust Global Trajectory Optimization," *IEEE Congress on Evolutionary Computation*, Inst. of Electrical and Electronics Engineers, Piscataway, NJ, 25–28 Sept. 2007, pp. 2056–2063.